Ultraviolet Detection of the Binary Companion to the Type IIb SN 2001ig

Item Type	Article
Authors	Ryder, Stuart D.; Dyk, Schuyler D. Van; Fox, Ori D.; Zapartas, Emmanouil; Mink, Selma E. de; SMITH, NATHAN; Brunsden, Emily; Bostroem, K. Azalee; Filippenko, Alexei V.; Shivvers, Isaac; Zheng, WeiKang
Citation	Stuart D. Ryder et al 2018 ApJ 856 83
DOI	10.3847/1538-4357/aaaf1e
Publisher	IOP PUBLISHING LTD
Journal	ASTROPHYSICAL JOURNAL
Rights	© 2018. The American Astronomical Society. All rights reserved.
Download date	27/08/2022 11:44:16
Item License	http://rightsstatements.org/vocab/InC/1.0/
Version	Final published version
Link to Item	http://hdl.handle.net/10150/632623

Ultraviolet Detection of the Binary Companion to the Type IIb SN 2001ig

Stuart D. Ryder[1] , Schuyler D. Van Dyk[2] , Ori D. Fox[3] , Emmanouil Zapartas[4], Selma E. de Mink[4] , Nathan Smith[5],
Emily Brunsden[6], K. Azalee Bostroem[7], Alexei V. Filippenko[8,9] , Isaac Shivvers[8] , and WeiKang Zheng[8]

[1] Australian Astronomical Observatory, 105 Delhi Road, North Ryde, NSW 2113, Australia; sdr@aao.gov.au
[2] Caltech/IPAC, Mailcode 100-22, Pasadena, CA 91125, USA
[3] Space Telescope Science Institute, 3700 San Martin Drive, Baltimore, MD 21218, USA
[4] Anton Pannekoek Institute for Astronomy, University of Amsterdam, Science Park 904, 1098 XH, Amsterdam, The Netherlands
[5] Steward Observatory, University of Arizona, Tucson, AZ 85721, USA
[6] Department of Physics, University of York, Heslington, York YO10 5DD, UK
[7] Department of Physics, University of California, Davis, CA 95616, USA
[8] Department of Astronomy, University of California, Berkeley, CA 94720-3411, USA
[9] Miller Senior Fellow, Miller Institute for Basic Research in Science, University of California, Berkeley, CA 94720, USA

Abstract

We present HST/WFC3 ultraviolet imaging in the F275W and F336W bands of the Type IIb SN 2001ig at an age of more than 14 years. A clear point source is detected at the site of the explosion, with $m_{\mathrm{F275W}} = 25.39 \pm 0.10$ and $m_{\mathrm{F336W}} = 25.88 \pm 0.13$ mag. Despite weak constraints on both the distance to the host galaxy NGC 7424 and the line-of-sight reddening to the supernova, this source matches the characteristics of an early B-type main-sequence star with $19{,}000 < T_{\mathrm{eff}} < 22{,}000$ K and $\log(L_{\mathrm{bol}}/L_\odot) = 3.92 \pm 0.14$. A BPASS v2.1 binary evolution model, with primary and secondary masses of 13 $M_\odot$ and 9 $M_\odot$, respectively, is found to simultaneously resemble, in the Hertzsprung–Russell diagram, both the observed location of this surviving companion, and the primary star evolutionary endpoints for other Type IIb supernovae. This same model exhibits highly variable late-stage mass loss, as expected from the behavior of the radio light curves. A Gemini/GMOS optical spectrum at an age of 6 years reveals a narrow He II λ4686 emission line, indicative of continuing interaction with a dense circumstellar medium at large radii from the progenitor. We review our findings on SN 2001ig in the context of binary evolution channels for stripped-envelope supernovae. Owing to the uncrowded nature of its environment in the ultraviolet, this study of SN 2001ig represents one of the cleanest detections to date of a surviving binary companion to a Type IIb supernova.

Key words: binaries: close – binaries: general – stars: evolution – stars: massive – supernovae: general – supernovae: individual (SN 2001ig)

Supporting material: data behind figure

1. Introduction

Core-collapse supernovae (CCSNe) can result when massive stars exhaust their available fuel and the cores collapse under their own weight, thereby releasing enough potential energy to eject their outer layers (Bethe et al. 1979; Woosley et al. 2002). Stripped-envelope SNe (SESNe) are a subset of CCSNe with progenitor stars that have lost most or all of their outer hydrogen envelope, and in some cases even their helium envelopes (e.g., Filippenko 1997).

Type IIb supernovae (SNe) are distinguished by their initially strong H lines that fade away over the course of weeks to months (Filippenko 1988, 1997; Filippenko et al. 1993; Gal-Yam 2016). This moderate amount of observed H is usually interpreted as an intermediate case between the H-rich SNe IIP/IIL and H-poor SNe Ib/c, presumably reflecting an increase in stripping of the stellar envelope from IIP/L → IIb → Ib → Ic. Recent evidence, however, appears to demonstrate that SNe IIb are spectroscopically distinct from SNe Ib/c at all epochs (Liu et al. 2016). Further indications that SNe IIb form a separate channel from SNe IIP/IIL come from their low ejecta masses (Lyman et al. 2016), together with radiative transfer models of their spectra (Dessart et al. 2012).

At least two scenarios can account for the stripping of the progenitor star's envelope prior to its eventual demise in a SN explosion (for both SNe IIb and Ib/c subclasses). Stellar winds accompanied by extreme or eruptive mass loss can shed significant amounts of gas over the lifetime of massive stars, (e.g., Heger et al. 2003; Smith & Owocki 2006); however, the mass loss rates for these tend to be overestimated (Smith 2014). Alternatively (or additionally), interaction with a massive binary companion can transport the H-rich outer layers into the circumstellar medium (CSM; e.g., Podsiadlowski et al. 1993; Eldridge et al. 2008; Claeys et al. 2011; Hirai et al. 2014). These two scenarios allow for a large range of potential progenitor systems and thus of possible companions at the moment of explosion, as summarized by Zapartas et al. (2017a). In scenarios that include a surviving binary companion, most models predict that this survivor should be a relatively unevolved, hot main-sequence star (Eldridge et al. 2015).

Identification of the progenitor system can provide important constraints on the mass loss scenarios and theoretical evolution of massive stars. While SNe IIb constitute only ∼10% of local CCSNe (Smith et al. 2011; Shivvers et al. 2017), they are one of the best-studied subclasses, including several progenitor detections. SN 1993J in M81 attracted considerable interest in part owing to its proximity (3.6 Mpc), which enabled the detection of not just the progenitor star (Aldering et al. 1994; Van Dyk et al. 2002) but also a putative early B-type supergiant companion star (Maund et al. 2004; Fox et al. 2014). Progenitor stars have also been identified in pre-explosion images of the

Type IIb SNe 2008ax (Crockett et al. 2008; Folatelli et al. 2015), 2011dh (Maund et al. 2011; Van Dyk et al. 2011, 2013), 2013df (Van Dyk et al. 2014), and 2016gkg (Kilpatrick et al. 2017; Tartaglia et al. 2017; Bersten et al. 2018), while searches for a binary companion to SN 2011dh are inconclusive (Folatelli et al. 2014; Maund et al. 2015). The relatively low initial masses inferred from these SNe IIb progenitors, which overlap with the progenitor mass range of SNe IIP (Smartt 2009), further complicate the hypothesis that SNe IIb form a transition from normal SNe IIP/IIL to SNe Ibc with increasing initial mass and/or mass loss rate.

The mass loss and progenitor properties can also be constrained indirectly. The interaction of the expanding SN blast wave with a pre-existing CSM consisting of material shed by the stellar progenitor gives rise to multi-wavelength emission, including X-ray inverse Compton scattering and radio continuum synchrotron radiation. Multi-frequency radio light curves on timescales of hours to years enable the reconstruction of the progenitor star's mass loss history centuries into the past. With a measured or assumed wind speed, the mass loss rate can be calculated as a function of time to narrow down potential progenitors (Weiler et al. 2002; Horesh et al. 2013; Smith 2014).

The Type IIb SN 2001ig was discovered visually by Evans et al. (2001) on 2001 December 10.43 UT on the outskirts of the nearby late-type spiral galaxy NGC 7424, but received surprisingly little optical study despite reaching 12th magnitude (Bembrick et al. 2002). Silverman et al. (2009) published 12 optical spectra, Maund et al. (2007) presented 3 epochs of optical spectropolarimetry, and Ryder et al. (2006) showed a late-time spectrum, all taken within the first year after explosion. Silverman et al. (2009), Maund et al. (2007), and Shivvers et al. (2013) pointed out both the observed similarities and differences between SN 2001ig and SN 1993J. Shivvers et al. (2013) further compared SN 2001ig in the nebular phase with SN 2011dh. Had there been an optical light curve for SN 2001ig, particularly at early times, it would have been evident from the timing of the decline from the initial cooling phase whether SN 2001ig was more like SN 1993J, with its extended-envelope progenitor, or SN 2011dh, arising from a somewhat more compact star.

SN 2001ig was detected in X-rays with *Chandra* (Schlegel & Ryder 2002), yet the most complete coverage of all was at radio wavelengths. Following the initial detection within 5 days of discovery, Ryder et al. (2004) presented almost 2 years worth of data from the Australia Telescope Compact Array (ATCA) and the Very Large Array (VLA) at frequencies between 1.4 and 22.5 GHz. Fitting the multi-frequency light curves enabled them to infer a mass loss rate from the progenitor of $\sim 2 \times 10^{-5}\,M_\odot\,\mathrm{yr}^{-1}$, for a wind velocity of $10\,\mathrm{km\,s}^{-1}$.

There are no pre-explosion images of NGC 7424 of sufficient depth or resolution to enable a direct identification of the progenitor to SN 2001ig. The radio light curves, however, exhibited regular modulations, with a period of ~ 150 days between peaks, which Ryder et al. (2004) attributed to "sculpting" of the CSM by a binary companion. Ryder et al. (2006) imaged the location of SN 2001ig with the Gemini Multi-Object Spectrograph (GMOS) on the Gemini South 8 m telescope and identified an optical counterpart in g' and r' data, consistent with the presence of a surviving supergiant

companion of spectral type late-B through late-F, depending on the extinction assumed.

Soderberg et al. (2006) drew attention to several similarities between the radio light curves of SN 2001ig and those of the broad-lined Type Ic SN 2003bg, including the strength of the modulations and their period. Since the likelihood of these two distinct SN subtypes having almost the same binary progenitor system properties (orbital period, mass ratio) that would give rise to such similar CSM structures must be extremely small, Soderberg et al. (2006) favored instead a scenario in which both SN 2001ig and SN 2003bg have single Wolf–Rayet star progenitors that undergo quasi-periodic episodes of enhanced mass loss. Kotak & Vink (2006) suggested that S Doradus-type variations, as seen in luminous blue variables (LBVs), could be one such mechanism. Ben-Ami et al. (2015) analyzed early-time ultraviolet (UV) spectra obtained with the *Hubble Space Telescope* (*HST*) of four SNe IIb, including SN 2001ig. In contrast to SNe 1993J, 2011dh, and 2013df, the UV spectra of SN 2001ig showed a quite weak continuum, and strong reverse-fluorescence features more akin to those of Type Ia SNe, consistent with a high radioactive ^{56}Ni mass and a compact progenitor object.

As part of *HST* program GO-14075 (PI: O. Fox), we used the Wide Field Camera 3 (WFC3) to search for surviving binary companions to nearby SESNe in the UV. In Zapartas et al. (2017b) we placed deep upper limits on the mass of a binary companion to the broad-lined Type Ic SN 2002ap, and used binary population synthesis models to rule out the 40% of SESN channels that would have resulted in a surviving main-sequence companion more massive than this. Section 2.1 presents our new *HST*/WFC3 UV observations of SN 2001ig, while Section 2.2 describes previously unpublished Gemini South/GMOS spectroscopy from 2007. We outline our photometric results in Section 3.1 and our spectroscopic results in Section 3.2. Our interpretation of these in terms of a binary progenitor system is in Section 4 and our conclusions are summarized in Section 5. We note that NGC 7424 has also recently served as host to the Type II SN 2017bzb (Morrell et al. 2017).

2. Observations

2.1. HST Imaging

We imaged the site of SN 2001ig with WFC3/UVIS on 2016 April 28 UT (14.4 years after explosion) in bands F275W and F336W, with total exposures of 8694 s and 2920 s, respectively. The exposures were line-dithered, to improve image quality and resolution and to mitigate against hot pixels and cosmic ray hits, and post-flashed to help mitigate against charge-transfer efficiency (CTE) losses. The images had been processed through the standard pipeline at the Space Telescope Science Institute (STScI) before we obtained them from the Mikulski Archive for Space Telescopes (MAST). Specifically, the individual *flt* frames had been corrected for CTE losses. We then ran these corrected *flc* frames through the routine AstroDrizzle within PYRAF, to create final image mosaics in each band.

We identified the SN on the WFC3 images by astrometrically aligning the F336W image mosaic to the GMOS g' image obtained in 2004 under very good seeing conditions (0″.35–0″.45 FWHM; Ryder et al. 2006). Using the 11 stars in common between the 2 images as astrometric fiducials, we
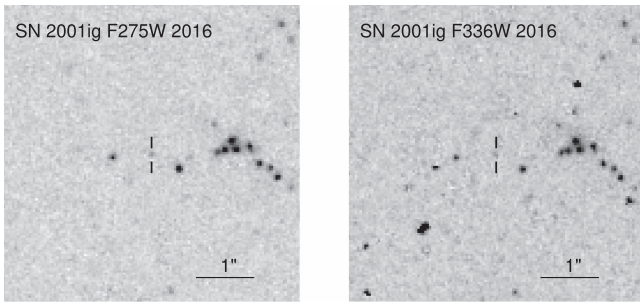
Figure 1. (Left): a portion of the *HST* WFC3/UVIS F275W image from 2016 obtained as part of GO-14075; the exact site of SN 2001ig is indicated with tick marks. (Right): the same, but in F336W. Some cosmic ray hits have not been completely removed from the image in the right panel. North is up and east is to the left, in both panels.
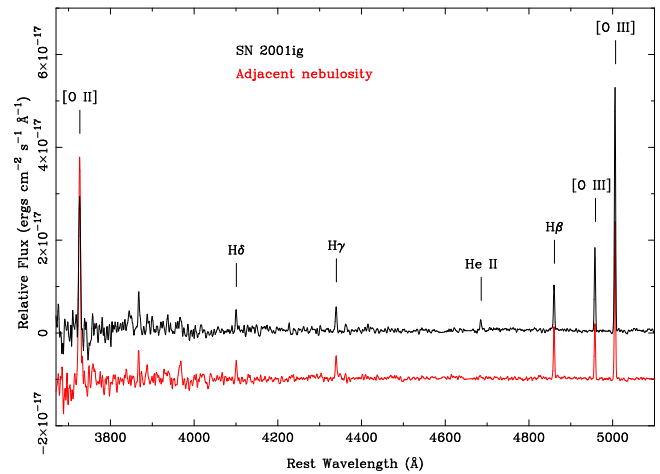

Figure 2. Spectra from Gemini/GMOS in 2007 of the site of SN 2001ig (black), and the nebulosity adjacent to this (red), with the latter displaced vertically to assist comparison. Major emission features are marked. Note the presence of He II λ4686 emission only in the spectrum of the SN 2001ig site. The data used to create this figure are available.

identify a source corresponding to the location of SN 2001ig with an rms uncertainty of 0.32 UVIS pixel (12.7 milliarcsec). The location of the source in both the F275W and F336W images is indicated in Figure 1.

We measured photometry for this detected source by inputting the individual *flc* frames into Dolphot (Dolphin 2000). We ran this routine with parameters set to FitSky = 3, RAper = 8, and InterpPSFlib = 1, using the TinyTim model point-spread functions (PSFs). By running the frames first through AstroDrizzle, cosmic ray hits in the frames had also been flagged, which is important for accurate aperture correction. As a result, we found for the identified source $m_{F275W} = 25.39 \pm 0.10$ and $m_{F336W} = 25.88 \pm 0.13$ mag. These are robust detections of a point-like source at the position of SN 2001ig with signal-to-noise ratios of ~12 and 9, respectively. The object identifier in the Dolphot output was equal to 1 for both bands, and the sharpness parameter was quite low: −0.011 and −0.007 for F275W and F336W, respectively.

2.2. GMOS Spectroscopy

Deep optical spectroscopy of the site of SN 2001ig was obtained with the Gemini South Telescope using GMOS (Hook et al. 2004) as part of program GS-2006B-Q-11 (PI: S. Ryder). A total of 5 hr on-source integration was obtained over the course of two nights in 2007, July 18 and November 6 UT, in photometric IQ20 (seeing <0″6) conditions. The B600 grating was used with a 0″5 slit, giving a nominal resolution $R \sim 1700$.

The GMOS optical spectral data were reduced using the GMOS tasks in V1.10 of the GEMINI package within IRAF. A master bias frame, constructed by averaging with 3σ clipping a series of bias frames, was subtracted from all raw images. Images of a Cu–Ar lamp spectrum were used to wavelength calibrate the science images and straighten (rectify) them along the spatial dimension, while images of a quartz-halogen lamp spectrum helped correct for sensitivity variations within and between the original e2v CCDs.

The two-dimensional data sets from each night were reduced separately, then registered spatially and in wavelength space before being coadded. By comparing continuum sources in the resultant spectral image with field stars visible in GMOS images from 2004 (Ryder et al. 2006, their Figure 1), the rows containing emission from SN 2001ig could be identified. The flux within an aperture 0″9 wide centered on the SN location was extracted, together with an adjacent but not overlapping

aperture of the same width to represent the nebular emission from the environment of SN 2001ig. Observations of the spectrophotometric standard star LTT 9239 (Hamuy et al. 1994) with the same instrument setup and similar airmass to that of the SN 2001ig observations enabled a system response function to be derived and applied over the wavelength range 370–650 nm, as well as the removal of telluric features in the extracted spectra. Figure 2 compares the spectra at the location of SN 2001ig and the adjacent nebulosity.

3. Analysis

3.1. Photometric Properties of the Companion

The total reddening toward SN 2001ig is uncertain, but we expect it to be relatively low. The use of quite a narrow slit in order to minimize background contamination of the SN 2001ig spectrum over several hours of integration (and thus a large range in slit parallactic angle traversed) precludes the use of the Balmer decrement to estimate the extinction toward adjacent H II regions because of slit losses.[10] The contribution from the Galactic foreground extinction is $A_V = 0.029$ mag (Schlafly & Finkbeiner 2011, via the NASA/IPAC Extragalactic Database, NED). Silverman et al. (2009) measured from their highest resolution spectrum an equivalent width of $\lesssim 0.1$ Å for the Na I D feature and concluded that the contribution from the host galaxy was likely no greater than the Galactic contribution; they also noted that Maund et al. (2007) did require some additional reddening, beyond the Galactic component, to account for the observed optical polarization of the SN signal. We therefore assume that the host reddening is essentially equivalent to the Galactic reddening; the total extinction to the SN site is thus $A_V = 0.06$ mag. We further assume a Cardelli et al. (1989) reddening law with $R_V = 3.1$.

Regarding the metallicity at the site of SN 2001ig, Modjaz et al. (2011) found that the oxygen abundance $12 + \log(O/H)$ is between 8.27 and 8.53, depending on the abundance diagnostic used. Assuming that solar abundance is 8.7 (e.g.,

---

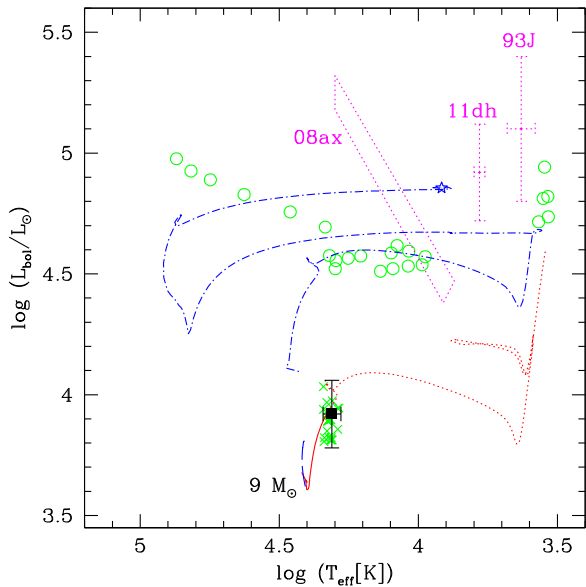[10] See http://www.gemini.edu/?q=node/11212.

Figure 3. Hertzsprung–Russell diagram showing the locus of the point source detected at the site of SN 2001ig (solid symbol). Its properties are inferred from comparison of the observed *HST* ultraviolet photometry with stellar atmosphere models for main-sequence stars at metallicity [Fe/H] = −0.25 (Castelli & Kurucz 2003). Shown for comparison in red is a single-star evolutionary track at $9\,M_\odot$ for this same metallicity from MIST. Also shown are the locations of the secondaries (green crosses) that are consistent with the detected point source (to within the uncertainties) of 24 BPASS v2.1 binary evolution models, as well as the corresponding endpoints of the model primaries (green open circles). For reference, the loci of the progenitors of SN 1993J (Aldering et al. 1994; Van Dyk et al. 2002), SN 2011dh (Maund et al. 2011; Van Dyk et al. 2011), and SN 2008ax (Folatelli et al. 2015) are shown in magenta (dotted lines). Additionally, for comparison in blue is a BPASS binary evolution model with a primary (dashed–dotted line) and secondary (long-dashed line) of initial masses 13 and $9\,M_\odot$, respectively, and an initial period of 400 days; the terminus of the primary track is indicated with a star.

Scott et al. 2009), the metallicity appears to be around 1/3–2/3 solar at the location of SN 2001ig.

We analyzed the photometry in the F275W and F336W bands using Castelli & Kurucz (2003) model atmospheres for main-sequence stars at the appropriate metallicity ([Fe/H] = −0.25) and reddened by the amount assumed above. We find that the photometry is consistent with an early B-type star with an effective temperature $T_{\rm eff} = 19{,}000$–22,000 K. The corresponding brightness in *V* of these models is then 27.11–27.35 mag.

The distance to the host galaxy NGC 7424 is not well determined. However, it likely sits somewhere between 10.9 (Böker et al. 2002) and 11.5 Mpc (Tully 1988; Soria et al. 2006), depending on the value of the Hubble constant assumed, with a corresponding distance modulus of 30.19–30.30 mag. If the detected source is a main-sequence star, its absolute magnitude is then in the range $M_V = -3.25$ to −2.90. For the above range in $T_{\rm eff}$, at the assumed metallicity, the *V*-band bolometric correction is −1.82 to −2.16 mag (Paxton et al. 2011, 2013, 2015; Choi et al. 2016). This would imply that the bolometric magnitude is $M_{\rm bol} = -5.06 \pm 0.35$ mag, which for $M_{\rm bol}(\odot) = 4.74$ mag corresponds to a bolometric luminosity $\log(L_{\rm bol}/L_\odot) = 3.92 \pm 0.14$.

In Figure 3 we have placed this inferred $T_{\rm eff}$ and $L_{\rm bol}$ on a Hertzsprung–Russell diagram (HRD). For comparison we show a MIST single-star evolutionary track at initial mass $9\,M_\odot$ at metallicity [Fe/H] = −0.25 (Paxton et al. 2011, 2013, 2015; Choi et al. 2016); the track is shown as a solid line up to the data point and then extrapolated as a dotted line for the remainder of

the track. The locus of the detected source agrees with a star at this mass nearing the terminal-age main-sequence (TAMS).

We have found 24 binary evolution models (out of a total of 12,678 models generated at this metallicity) from BPASS[11] version 2.1 (Eldridge et al. 2017) for which the secondary star tracks place them within the uncertainties of the detected object at the time their primaries explode. In Figure 3 we also show as green circles the endpoints of the tracks of the corresponding model primaries, i.e., when carbon burning ends, and core-collapse is imminent. However, in nearly all of these cases the primary star endpoint is either cooler (appearing as a red supergiant) or hotter than expected for SN IIb progenitors, including SN 1993J and SN 2011dh (to which SN 2001ig's early spectral evolution is most similar: Ryder et al. 2006; Shivvers et al. 2013), or even SN 2008ax. This is evident also in Figure 21 of Eldridge et al. (2017), which shows the BPASS models for Type IIb SNe favoring blue or red supergiant progenitors over yellow supergiants.

We found one BPASS model with a secondary of initial mass $9\,M_\odot$ (similar to what we infer for the detected source), a primary of initial mass $13\,M_\odot$ (see Figure 3), and an initial orbital period of 400 days. Although the agreement is not perfect, the endpoint of this model has the secondary on the HRD at a locus not far ($\sim 2\sigma$) from that of the detected object; while the track of the $13\,M_\odot$ primary ends at a $T_{\rm eff}$ and $L_{\rm bol}$ that is not too dissimilar from the locus of the progenitor of SN 2011dh, which had an initial mass 10–$19\,M_\odot$ (Maund et al. 2011; Van Dyk et al. 2011); or that for SN 1993J (Van Dyk et al. 2002), whose progenitor mass was in the range 13–$22\,M_\odot$.

This particular BPASS model terminates with a primary core mass of $\sim 3.5\,M_\odot$ and with $\sim 0.04\,M_\odot$ of H remaining. These numbers are quite similar to those yielded by the independent binary evolution models of Ouchi & Maeda (2017) for a secondary-to-primary mass ratio of $0.6 < q < 0.8$, initial orbital period $200 < P < 600$ days, and a low efficiency ($f \approx 0$) of mass accretion from the primary onto the secondary. The blue loop in Figure 3 is similar to that seen in the models of Yoon et al. (2017) for Type IIb interacting binary progenitors with periods of a few hundred days, and masses closer to $10\,M_\odot$ than $20\,M_\odot$. These primaries leave low-mass helium-rich remnants (roughly 2–$4\,M_\odot$) that undergo a second mass transfer stage when they swell up again during helium shell-burning. Building on the convention of Dewi et al. (2002) they refer to this as "Case EBB/LBB" mass transfer.

The primary in this BPASS model also appears to experience a sudden increase in mass loss in the last $\sim 50{,}000$ years, with strongly variable mass loss over the final ~ 1700 years of the model. This appears to be a real effect, not simply an artifact of the model, and is due to late Roche lobe overflow of the He star primary onto the secondary, which changes the surface conditions and thus the assumed stellar wind mass loss rates (J. J. Eldridge 2017, private communication). Whether such fluctuations in mass loss occur in reality is yet to be proven, but would not be inconsistent with what was inferred for the progenitor from analysis of the radio observations of SN 2001ig (Ryder et al. 2004).

Note that we are suggesting here only that this particular model has properties that are consistent with that of a SN IIb progenitor system, not that this is the actual model for SN 2001ig. We caution that the endpoint for any given primary star mass depends much more heavily on the mass

---

[11] http://bpass.auckland.ac.nz/

loss rates assumed than on the parameters of the binary system. The relative fraction of primaries that finish up as blue supergiants rather than red supergiants increases with mass loss rate. Mass loss is a notoriously complex problem (e.g., Smith et al. 2011; Smith 2014; Renzo et al. 2017), and observations by Beasor & Davies (2016) suggest mass loss rates may evolve more steeply with luminosity than standard models predict. For reference, the BPASS models adopt mass loss rates for OB stars from the radiative transfer calculations of Vink et al. (2001), while for later types they employ the tabulation by de Jager et al. (1988) of empirical mass loss rates as a function of position within the HR diagram; in both cases these are then scaled appropriately for the metallicity of the star. Similarly, the Type IIb binary progenitor models of Yoon et al. (2017) use the MESA[12] code (Paxton et al. 2011), and the so-called "Dutch" scheme for mass loss, which is a hybrid of these and other mass loss prescriptions (Glebbeek et al. 2009). In none of these models, however, is the mass loss rate tied directly to a specific core- or shell-burning phase.

3.2. Spectroscopic Properties of the Companion

Figure 2 compares the extracted spectrum from the location of SN 2001ig with that of the adjacent nebulosity. The two are virtually identical, indicating some degree of probable foreground and/or background contamination of the SN+companion optical spectrum by this nebulosity. The one notable difference between them, however, is the clear detection (30σ) of emission from He II $\lambda 4686$ in the SN spectrum only. This narrow line (FWHM = $250\,\mathrm{km\,s^{-1}}$) has a flux ratio relative to the nearby Hβ line (thus independent of the reddening assumed) of 0.30 ± 0.03.

Nebular He II $\lambda 4686$ emission requires quite hard ionizing radiation, such as that from an active galactic nucleus, shocks, or X-ray binaries. It can also be the signpost of the hottest stars, in particular, Wolf–Rayet (WR) stars, albeit as a much broader feature owing to the fast, dense stellar winds (Crowther 2007). Nebular He II $\lambda 4686$ can also be seen without the other usual accompanying spectral features of WR stars, (e.g., López-Sánchez & Esteban 2010). WR stars are claimed to be the progenitors to some types of SESNe (Smartt 2009), including the Type IIb SN 2008ax (Crockett et al. 2008), although Folatelli et al. (2015) used post-explosion *HST* imaging to argue against a WR progenitor in that particular case.

Such weak and narrow He II $\lambda 4686$ emission was also seen to emerge in SN 2014C 1–2 years post-explosion (Milisavljevic et al. 2015; Anderson et al. 2017). This is also the interval during which SN 2014C apparently evolved from an ordinary SN Ib into a strongly interacting SN IIn-like event. In addition, both SN 1993J (Matheson et al. 2000) and SN 2013df (Maeda et al. 2015) underwent a spectral transformation after the first year, indicative of interaction with a dense CSM, albeit through the appearance of broad, flat-topped Hα and He I lines, rather than He II $\lambda 4686$. Transitory He II $\lambda 4686$ emission was also seen briefly at around 100 days in the Type Ibn SN 2006jc (Smith et al. 2008), coincident with the onset of dust formation in a dense CSM shell.

Optical spectroscopy by Milisavljevic et al. (2015), as well as radio observations by Anderson et al. (2017) and X-ray observations by Margutti et al. (2017), led to the conclusion that the progenitor of SN 2014C initially exploded into a low-

density cavity before eventually running into a dense, H-rich shell of material shed long before it exploded. Such delayed interaction has been seen previously in objects such as SN 1996cr (Bauer et al. 2008), as well as SN 1987A, which has slowly overtaken its dense, clumpy ring. Thus, it may be that this He II $\lambda 4686$ emission in SN 2001ig is a signpost of ongoing or renewed interaction with CSM much farther out than that probed by the radio emission. This would suggest that the SN 2001ig progenitor, like the case of SN 2014C, may have been intermediate between the more compact progenitor (with a less dense CSM) of SN 2011dh, and the more extended progenitor (and stronger CSM interaction) of SN 1993J.

4. Discussion

4.1. An Innocent Bystander?

While the object detected in the WFC3 images could simply be a chance alignment of an unrelated foreground/background source, this seems extremely unlikely for two reasons. First, the somewhat sparse distribution of detectable UV sources in Figure 1 makes this a rather low statistical probability; and second, it is just as unlikely that this contaminating source happens to show rare, narrow He II $\lambda 4686$ emission, rather than a much more common stellar continuum.

On the basis of ground-based optical imaging obtained in 2004, Ryder et al. (2006) suggested that this surviving companion was most likely a supergiant star, somewhere between a late-B (for $A_V \sim 1$ mag) to late-F (for $A_V = 0$ mag) spectral type. Our *HST* UV imaging taken 12 years later now indicates the companion is more likely to be a main-sequence B star with quite low extinction ($A_V = 0.06$ mag; Section 3.1). We found that the ($g'-r'$) color and ($u'-g'$) blue limit of the 2004 source were inconsistent with either a pure H II region or the nebular spectrum of SN 1993J at a similar age. It is quite likely that the source spectrum will have evolved since 2004, fading in the manner extrapolated for SN 2011dh by Maund et al. (2015), but perhaps rebrightening owing to ongoing or resumed CSM interaction as hinted at by the emergence of He II $\lambda 4686$ emission. Unfortunately, there has been very little photometric monitoring of SN 2001ig throughout its evolution to yield a meaningful light curve from which to extrapolate to such late times. We also consider the possibility that newly formed dust in the system may be either partially or fully obscuring the companion, and that our detection is a line-of-sight coincidence. In this case, mid-infrared emission may arise from dust warmed by the companion. The *Spitzer Space Telescope* serendipitously observed the position of SN 2001ig over several epochs spanning 2009 through 2016 (program IDs 61065, 10136, 11063), but no source is detected in a stack of these data. We estimate upper limits ($\approx 3\sigma$) of $<0.3\,\mu$Jy and $<0.7\,\mu$Jy to detection at 3.6 and 4.5 μm, respectively. Following techniques outlined in Dwek et al. (2017; their Figure 7), these limits constrain the possible dust mass, temperature, and radius (assuming a spherically symmetric geometry). If a B-type companion star ($\sim 10^{4.5}\,L_\odot$) is present, these *Spitzer* results can rule out the presence of the warmest dust at the innermost radius, but do allow for colder dust at larger radii. At these larger radii, however, a significantly larger dust mass (e.g., $>10^{-2}\,M_\odot$) would be required, which are not consistent with typical dust masses produced in binary interaction (Kochanek 2017).

---

[12] http://mesa.sourceforge.net

4.2. Binary Evolutionary Channel for the SN 2001ig Progenitor

The presence of a surviving stellar companion would imply that the progenitor star of SN 2001ig was in a binary system. Indeed, if that is the case, mass transfer onto the binary companion of the progenitor would have played an important role in the removal of almost all of its H-rich envelope, thus leading to a Type IIb SN event.

Zapartas et al. (2017a) provided theoretical predictions for the binary companions of all SESNe (including SNe IIb and SNe Ib/c). They found that in the majority of scenarios a binary companion star is expected at the moment of explosion. In most cases the companion still resides on the main-sequence, since it evolves on a longer timescale owing to its lower initial mass. In fact, our inferred mass of $\sim 9\,M_\odot$ for the companion of SN 2001ig coincides with the broad peak of the predicted mass distribution of main-sequence companions of all SESNe shown in Zapartas et al. (2017a).

Binary channels that originate from short-period systems (about $1 \lesssim \log P\,(\mathrm{days}) \lesssim 3$) have been suggested to result in compact SN IIb progenitors (Stancliffe & Eldridge 2009; Yoon et al. 2010; Bersten et al. 2012; Benvenuto et al. 2013; Folatelli et al. 2015; Yoon et al. 2017), with a thin H envelope of mass $\lesssim 0.15\,M_\odot$ (e.g., Yoon et al. 2017). In low-metallicity environments, weak stellar winds allow the thin remaining envelope to still be present when the progenitor explodes. The progenitors of these compact SNe IIb stay on the blue part of the HRD or are expected to end their lives as yellow supergiants (YSGs), as in the case of direct progenitor detections of SN 2011dh and SN 2013df. The BPASS model shown in Figure 3 follows such a scenario, having an initial period $\log P = 2.6$ and leaving $0.04\,M_\odot$ of H remaining on the progenitor at the moment of explosion.

Alternatively, wider initial orbits lead to more massive H envelopes (e.g., Yoon et al. 2017). Progenitors with an extended low-mass H envelope of ~ 0.1–$0.5\,M_\odot$ (Podsiadlowski et al. 1993; Woosley et al. 1994; Elmhamdi et al. 2006; Claeys et al. 2011) are expected to stay on the red part of the HRD. Claeys et al. (2011) found that extended SN IIb progenitors originate from almost equal-mass systems with $q = M_{\mathrm{accretor}}/M_{\mathrm{donor}} \gtrsim 0.7$–$0.8$ in initially wide orbits of $3 \lesssim \log P\,(\mathrm{days}) \lesssim 3.3$. Although they assume conservative mass transfer as their standard assumption, they also explored binary evolution for different mass transfer efficiencies to determine the uncertainty in how much mass is accreted by the companion star.

In the case of low efficiency, as expected in systems with wide orbits (e.g., Schneider et al. 2015), the inferred companion mass of $\sim 9\,M_\odot$ is relatively close to its birth mass. At the same time, the progenitor star initially should be somewhat more massive, since $q \gtrsim 0.7$, and will naturally form a He core of 3–$4\,M_\odot$, consistent with the ejecta mass of $\sim 1.15\,M_\odot$ inferred by Silverman et al. (2009). Thus, in the scenario of an extended SN IIb discussed here, the small difference in the evolutionary timescales owing to the similarity of the mass, as well as the possible absence of significant mass accretion onto the companion, results in only a limited rejuvenation of the companion (Hellings 1983, 1984). This could explain the fact that the detected companion appears to lie close to the TAMS, as seen in Figure 3.

A further consequence of possible non-conservative mass transfer is that SN IIb progenitors are expected to have a significant CSM around them just before the explosion,

corresponding to mass loss rates on the order of 10^{-5} to $10^{-4}\,M_\odot\,\mathrm{yr}^{-1}$, when averaged over the final 1000 years before the SN explosion (Ouchi & Maeda 2017), which is comparable to that inferred from the radio observations for SN 2001ig (Ryder et al. 2004). The CSM produced by the binary interaction could be the cause of the observed He II $\lambda 4686$ feature discussed in Section 3.2.

In summary, constraining the exact parameters of the original progenitor binary system is difficult owing to the lack of extensive optical photometric monitoring of SN 2001ig, or a direct detection of its progenitor. If SN 2001ig is similar to SN 2011dh, the expected YSG progenitor could have formed through mass transfer in a binary system with an initial period of a few hundred days, as is the case for the BPASS model shown in Figure 3. However, we cannot exclude the possibility of wider initial orbits, which would lead to more extended SN IIb progenitors.

5. Summary and Conclusions

We have obtained late-time UV imaging (over 14 years past explosion) of the site of SN 2001ig and identified in two separate filters a point source at the known location of the SN. Allowing for the uncertainties in distance and extinction toward the host galaxy, we find this source to be consistent with an early B-type main-sequence star with $T_{\mathrm{eff}} = 19,000$–$22,000$ K and a bolometric luminosity $\log(L_{\mathrm{bol}}/L_\odot) = 3.92 \pm 0.14$. We show that the evolutionary track of a BPASS model with a $9\,M_\odot$ secondary star passes near the TAMS on the HRD at about the same time that its $13\,M_\odot$ primary companion reaches a location on the HRD similar to those observed for the progenitors of SN 2011dh and SN 1993J. The growing number of surviving companions found in SNe IIb, coupled with their relatively low progenitor masses, weakens the case for massive single stars such as LBVs being the progenitors of most SNe IIb (Kotak & Vink 2006; Soderberg et al. 2006; Groh et al. 2013).

Although the progenitor star of SN 2001ig was never identified directly, we believe our detection of what is almost certainly the surviving companion in this model makes a strong case for a binary interaction scenario for SN 2001ig, leading to a partially stripped envelope and a dense CSM. A ground-based optical spectroscopic comparison of the location of SN 2001ig with its neighborhood at an age of almost 6 years reveals narrow He II $\lambda 4686$ emission, which we interpret as further evidence for interaction with this dense CSM.

SN 2001ig initially underwent strong interaction of the SN shock with the pre-existing CSM surrounding the progenitor for years after explosion, as revealed by its long-lived radio emission. This is a common property of SNe IIb, such as SN 1993J (Weiler et al. 2007), SN 2011dh (Horesh et al. 2013), and SN 2013df (Kamble et al. 2016). In the case of SN 2011dh, Maund et al. (2015) discussed the possibility of ongoing or renewed CSM interaction accounting for its observed late-time, *HST*-based optical spectral energy distribution. These authors pointed out that the UV emission from SN 2011dh, interpreted by Folatelli et al. (2014) as evidence for a binary companion, could instead be associated with such a potentially protracted CSM interaction, and recommended further monitoring at optical wavelengths with *HST* once this still relatively young SESN has faded enough to distinguish between these two possibilities. Similarly, additional optical imaging with *HST* in the future will be necessary to determine whether the UV

emission we have detected at the site of SN 2001ig is produced entirely by a surviving hot companion, or has a contribution from long-term, low-level CSM interaction.

ORCID iDs

Stuart D. Ryder ⓘ https://orcid.org/0000-0003-4501-8100
Schuyler D. Van Dyk ⓘ https://orcid.org/0000-0001-9038-9950
Ori D. Fox ⓘ https://orcid.org/0000-0003-2238-1572
Selma E. de Mink ⓘ https://orcid.org/0000-0001-9336-2825
Alexei V. Filippenko ⓘ https://orcid.org/0000-0003-3460-0103
Isaac Shivvers ⓘ https://orcid.org/0000-0003-3373-8047

References

Aldering, G., Humphreys, R. M., & Richmond, M. 1994, AJ, 107, 662
Anderson, G. E., Horesh, A., Mooley, K. P., et al. 2017, MNRAS, 466, 3648
Bauer, F. E., Dwarkadas, V. V., Brandt, W. N., et al. 2008, ApJ, 688, 1210
Beasor, E. R., & Davies, B. 2016, MNRAS, 463, 1269
Bembrick, C., Pearce, A., & Evans, R. 2002, IAUC, 7804, 2
Ben-Ami, S., Hachinger, S., Gal-Yam, A., et al. 2015, ApJ, 803, 40
Benvenuto, O. G., Bersten, M. C., & Nomoto, K. 2013, ApJ, 762, 74
Bersten, M., Folatelli, G., García, F., et al. 2018, Natur, 554, 497
Bersten, M. C., Benvenuto, O. G., Nomoto, K., et al. 2012, ApJ, 757, 31
Bethe, H. A., Brown, G. E., Applegate, J., & Lattimer, J. M. 1979, NuPhA, 324, 487
Böker, T., Laine, S., van der Marel, R. P., et al. 2002, AJ, 123, 1389
Cardelli, J. A., Clayton, G. C., & Mathis, J. S. 1989, ApJ, 345, 245
Castelli, F., & Kurucz, R. L. 2003, in IAU Symp. 210, Modelling of Stellar Atmospheres, ed. N. Piskunov, W. W. Weiss, & D. F. Gray (San Francisco, CA: PASP), A20
Choi, J., Dotter, A., Conroy, C., et al. 2016, ApJ, 823, 102
Claeys, J. S. W., de Mink, S. E., Pols, O. R., Eldridge, J. J., & Baes, M. 2011, A&A, 528, A131
Crockett, R. M., Eldridge, J. J., Smartt, S. J., et al. 2008, MNRAS, 391, L5
Crowther, P. A. 2007, ARA&A, 45, 177
de Jager, C., Nieuwenhuijzen, H., & van der Hucht, K. A. 1988, A&AS, 72, 259
Dessart, L., Hillier, D. J., Li, C., & Woosley, S. 2012, MNRAS, 424, 2139
Dewi, J. D. M., Pols, O. R., Savonije, G. J., & van den Heuvel, E. P. J. 2002, MNRAS, 331, 1027

Dolphin, A. E. 2000, PASP, 112, 1383
Dwek, E., Arendt, R. G., Fox, O. D., et al. 2017, ApJ, 847, 91
Eldridge, J. J., Fraser, M., Maund, J. R., & Smartt, S. J. 2015, MNRAS, 446, 2689
Eldridge, J. J., Izzard, R. G., & Tout, C. A. 2008, MNRAS, 384, 1109
Eldridge, J. J., Stanway, E. R., Xiao, L., et al. 2017, PASA, 34, e058
Elmhamdi, A., Danziger, I. J., Branch, D., et al. 2006, A&A, 450, 305
Evans, R. O., White, B., & Bembrick, C. 2001, IAUC, 7772, 1
Filippenko, A. V. 1988, AJ, 96, 1941
Filippenko, A. V. 1997, ARA&A, 35, 309
Filippenko, A. V., Matheson, T., & Ho, L. C. 1993, ApJL, 415, L103
Folatelli, G., Bersten, M. C., Benvenuto, O. G., et al. 2014, ApJL, 793, L22
Folatelli, G., Bersten, M. C., Kuncarayakti, H., et al. 2015, ApJ, 811, 147
Fox, O. D., Azalee, B. K., Van Dyk, S. D., et al. 2014, ApJ, 790, 17
Gal-Yam, A. 2016, in Handbook of Supernovae, ed. A. Alsabti & P. Murdin (Cham: Springer)
Glebbeek, E., Gaburov, E., de Mink, S. E., Pols, O. R., & Portegies Zwart, S. F. 2009, A&A, 497, 255
Groh, J. H., Meynet, G., & Ekström, S. 2013, A&A, 550, L7
Hamuy, M., Suntzeff, N. B., Heathcote, S. R., et al. 1994, PASP, 106, 566
Heger, A., Fryer, C. L., Woosley, S. E., Langer, N., & Hartmann, D. H. 2003, ApJ, 591, 288
Hellings, P. 1983, Ap&SS, 96, 37
Hellings, P. 1984, Ap&SS, 104, 83
Hirai, R., Sawai, H., & Yamada, S. 2014, ApJ, 792, 66
Hook, I. M., Jørgensen, I., Allington-Smith, J. R., et al. 2004, PASP, 116, 425
Horesh, A., Stockdale, C., Fox, D. B., et al. 2013, MNRAS, 436, 1258
Kamble, A., Margutti, R., Soderberg, A. M., et al. 2016, ApJ, 818, 111
Kilpatrick, C. D., Foley, R. J., Abramson, L. E., et al. 2017, MNRAS, 465, 4650
Kochanek, C. 2017, MNRAS, 471, 3283
Kotak, R., & Vink, J. S. 2006, A&A, 460, L5
Liu, Y.-Q., Modjaz, M., Bianco, F. B., & Graur, O. 2016, ApJ, 827, 90
López-Sánchez, Á. R., & Esteban, C. 2010, A&A, 516, A104
Lyman, J. D., Bersier, D., James, P. A., et al. 2016, MNRAS, 457, 328
Maeda, K., Hattori, T., Milisavljevic, D., et al. 2015, ApJ, 807, 35
Margutti, R., Kamble, A., Milisavljevic, D., et al. 2017, ApJ, 835, 140
Matheson, T., Filippenko, A. V., Ho, L. C., Barth, A. J., & Leonard, D. C. 2000, AJ, 120, 1499
Maund, J. R., Arcavi, I., Ergon, M., et al. 2015, MNRAS, 454, 2580
Maund, J. R., Fraser, M., Ergon, M., et al. 2011, ApJL, 739, L37
Maund, J. R., Smartt, S. J., Kudritzki, R. P., Podsiadlowski, P., & Gilmore, G. F. 2004, Natur, 427, 129
Maund, J. R., Wheeler, J. C., Patat, F., et al. 2007, ApJ, 671, 1944
Milisavljevic, D., Margutti, R., Kamble, A., et al. 2015, ApJ, 815, 120
Modjaz, M., Kewley, L., Bloom, J. S., et al. 2011, ApJL, 731, L4
Morrell, N., Shappee, B., Drout, M., & Dong, S. 2017, ATel, 1024, 1
Ouchi, R., & Maeda, K. 2017, ApJ, 840, 90
Paxton, B., Bildsten, L., Dotter, A., et al. 2011, ApJS, 192, 3
Paxton, B., Cantiello, M., Arras, P., et al. 2013, ApJS, 208, 4
Paxton, B., Marchant, P., Schwab, J., et al. 2015, ApJS, 220, 15
Podsiadlowski, P., Hsu, J. J. L., Joss, P. C., & Ross, R. R. 1993, Natur, 364, 509
Renzo, M., Ott, C. D., Shore, S. N., & de Mink, S. E. 2017, A&A, 603, A118
Ryder, S. D., Murrowood, C. E., & Stathakis, R. A. 2006, MNRAS, 369, L32
Ryder, S. D., Sadler, E. M., Subrahmanyan, R., et al. 2004, MNRAS, 349, 1093
Schlafly, E. F., & Finkbeiner, D. P. 2011, ApJ, 737, 103
Schlegel, E. M., & Ryder, S. 2002, IAUC, 7913, 1
Schneider, F. R. N., Izzard, R. G., Langer, N., & de Mink, S. E. 2015, ApJ, 805, 20
Scott, P., Asplund, M., Grevesse, N., & Sauval, A. J. 2009, ApJL, 691, L119
Shivvers, I., Mazzali, P., Silverman, J. M., et al. 2013, MNRAS, 436, 3614
Shivvers, I., Modjaz, M., Zheng, W., et al. 2017, PASP, 129, 054201
Silverman, J. M., Mazzali, P., Chornock, R., et al. 2009, PASP, 121, 689
Smartt, S. J. 2009, ARA&A, 47, 63
Smith, N. 2014, ARA&A, 52, 487
Smith, N., Foley, R. J., & Filippenko, A. V. 2008, ApJ, 680, 568
Smith, N., Li, W., Filippenko, A. V., & Chornock, R. 2011, MNRAS, 412, 1522
Smith, N., & Owocki, S. P. 2006, ApJL, 645, L45
Soderberg, A. M., Chevalier, R. A., Kulkarni, S. R., & Frail, D. A. 2006, ApJ, 651, 1005
Soria, R., Kuncic, Z., Broderick, J. W., & Ryder, S. D. 2006, MNRAS, 370, 1666

Stancliffe, R. J., & Eldridge, J. J. 2009, MNRAS, 396, 1699

Tartaglia, L., Fraser, M., Sand, D. J., et al. 2017, ApJL, 836, L12

Tully, R. B. 1988, Nearby Galaxies Catalog (Cambridge: Cambridge Univ. Press)

Van Dyk, S. D., Garnavich, P. M., Filippenko, A. V., et al. 2002, PASP, 114, 1322

Van Dyk, S. D., Li, W., Cenko, S. B., et al. 2011, ApJL, 741, L28

Van Dyk, S. D., Zheng, W., Clubb, K. I., et al. 2013, ApJL, 772, L32

Van Dyk, S. D., Zheng, W., Fox, O. D., et al. 2014, AJ, 147, 37

Vink, J. S., de Koter, A., & Lamers, H. J. G. L. M. 2001, A&A, 369, 574

Weiler, K. W., Panagia, N., Montes, M. J., & Sramek, R. A. 2002, ARA&A, 40, 387

Weiler, K. W., Williams, C. L., Panagia, N., et al. 2007, ApJ, 671, 1959

Woosley, S. E., Eastman, R. G., Weaver, T. A., & Pinto, P. A. 1994, ApJ, 429, 300

Woosley, S. E., Heger, A., & Weaver, T. A. 2002, RvMP, 74, 1015

Yoon, S.-C., Dessart, L., & Clocchiatti, A. 2017, ApJ, 840, 10

Yoon, S.-C., Woosley, S. E., & Langer, N. 2010, ApJ, 725, 940

Zapartas, E., de Mink, S. E., Izzard, R. G., et al. 2017a, A&A, 601, A29

Zapartas, E., de Mink, S. E., Van Dyk, S. D., et al. 2017b, ApJ, 842, 125